

## Thermal Properties of Polysilylenes

Manika Varma-Nair, Jinlong Cheng, Yimin Jin, and Bernhard Wunderlich\*

*Department of Chemistry, University of Tennessee, Knoxville, Tennessee 37996-1600, and Chemistry Division of Oak Ridge National Laboratory, Oak Ridge, Tennessee 37831-6197**Received March 5, 1991; Revised Manuscript Received April 16, 1991*

**ABSTRACT:** Quantitative thermal analysis was carried out for poly(dimethylsilylene) (PDMSi), poly(dipentylsilylene) (PDPSi), poly(dihexylsilylene) (PDHSi), and poly(ditetradecylsilylene) (PTDSi). Heat capacities were determined from 160 K to just below the decomposition temperatures. The ATHAS computation scheme was used to compute the "vibration-only" heat capacities,  $C_p$ , from 0.1 to 1000 K by fitting the experimental  $C_p$  below the glass transition temperature to an approximate vibrational spectrum. The  $C_p$  of the liquid was determined from an empirical addition scheme. A glass transition temperature,  $T_g$ , could be detected for PDPSi and PDHSi at 227.4 and 220.5 K, respectively, with the corresponding values for  $\Delta C_p$  of 47.7 and 37.9 J/(K mol). For PTDSi a glass transition is suggested at  $\approx 250$  K from a discussion of the heat capacity. For PDPSi there is only a small  $\Delta S_d$  [4 J/(K mol)]. In PDHSi and PTDSi, the observed endotherms lead to values of  $\Delta S_d$  of 46 and 119 J/(K mol) and account for about half of the maximum possible conformations participating in disordering. Polarizing microscopy revealed the change of the condis crystals to an isotropic state for PDPSi, PDHSi, and PTDSi at 518, 533, and 483 K, respectively. No prominent endotherm was observed in this temperature range. The short-side-chain homologue PDMSi reveals no glass transition or disordering transition and decomposes starting from 520 K.

## Introduction

Polysilylenes are unique linear macromolecules as their backbones consist entirely of silicon atoms. Attached to each Si atom are hydrocarbon pendant groups. The symmetrically substituted polysilylenes have gained importance in the last few years due to their interesting properties, such as  $\sigma$  conjugation and thermochromic and piezochromic transitions and a variety of potential applications such as photoconductors and photoresists.<sup>1-4</sup> The most extensively studied member of this class is poly(dihexylsilylene) (PDHSi), which has been investigated by UV,<sup>1-3</sup> IR,<sup>1,3</sup> and Raman spectroscopy,<sup>1,3,4</sup> by X-ray<sup>1,5</sup> and electron diffraction,<sup>5</sup> and by NMR.<sup>6,7</sup> The solid-state structures and the order-disorder phase transitions have also been reported for the lower homologues: poly(dimethylsilylene) (PDMSi),<sup>8</sup> poly(diethylsilylene) (PDESi),<sup>9</sup> poly(dipropylsilylene) (PDPrSi),<sup>9</sup> poly(dibutylsilylene) (PDBSi),<sup>10</sup> and poly(dipentylsilylene) (PDPSi).<sup>10</sup> In a recent review article,<sup>11</sup> all available information on the structure and phase transitions of the various polysilylenes was collected. All the polysilylenes with the exception of PDMSi are known to exhibit a first-order transition in the temperature range of 310–410 K in which the polymer is converted from a well-ordered phase to a phase with intramolecular disorder, but retains a high degree of intermolecular order.<sup>11</sup> Above their respective disordering transitions PDESi, PDBSi, PDPSi, and PDHSi all exhibit a large degree of motion in both the backbone and the side chains.<sup>5,6,10</sup> Differential scanning calorimetry (DSC) of PDMSi showed several small endotherms, attributed to the introduction of defects.<sup>8</sup> A small endothermic transition at 433 K was shown to probably be caused by a change of the packing of the molecules from monoclinic to hexagonal. The second small endotherm at 493 K may involve some conformational disordering.<sup>8</sup> It will be shown in this paper that the small endotherms observed in PDMSi probably represent only a change in the packing of the molecules while no large-scale conformational disordering can take place as was suggested before.<sup>8</sup>

The main purpose of the present research was the determination of the heat capacities of PDMSi, PDPSi, PDHSi, and poly(ditetradecylsilylene) (PTDSi) from 160 K to their respective decomposition temperatures. The

Advanced Thermal Analysis System (ATHAS) is used to compute heat capacities for the solid materials and empirically predict heat capacities in the liquid states. From the knowledge of the heat capacities of these two limiting states it is possible to understand the thermodynamics of this unique class of polymers. Furthermore, conclusions can be drawn about the disorder and motion in the mesophases of these polymers. In addition to the calorimetry, thermogravimetry and optical microscopy were carried out for general analysis.

## Experimental Section

**Samples.** The sample of PDMSi was obtained from the Union Carbide Corp. The other polymers, PDPSi, PDHSi, and PTDSi, were obtained through the courtesy of Dr. R. D. Miller of IBM Almaden Research Center, San Jose, CA. While no information was available on the molecular masses of PDMSi and PTDSi, PDPSi and PDHSi had high molecular masses of  $M_w = 1.69 \times 10^6$  and  $1.04 \times 10^6$ , respectively. All samples were white in color. PDMSi was a powder, while the rest were sticky in nature. PDMSi was dried in a desiccator for 48 h, while the rest were used as such.

**Instruments and Experiments.** All phase transition measurements were performed with a Perkin-Elmer DSC-7. Mechanical refrigeration was used to cool to 210 K and both the temperature and heat of fusion were calibrated by using standard materials (tin, indium, *p*-nitrotoluene, and *n*-dodecane). Typical sample masses were 15–20 mg; all measurements were carried out with a heating rate of 10 K/min. Base lines were set in accord with the computed heat capacities. Areas were determined by use of the software supplied by Perkin-Elmer. Heat capacity measurements from 140 K were carried out on a TA (Du Pont) 2100 thermal analyzer modified especially to carry out the low-temperature measurement.<sup>12</sup> The temperature calibration was carried out with cyclohexane, benzoic acid, naphthalene, tin, potassium nitrite, acetone, water, and indium. In addition, the heat capacity data were corrected for temperature lag, asymmetry of the three measuring positions, and heating rate with the computer program developed in our laboratory. Details of the techniques are described in ref 12. Heat capacity measurements of sapphire ( $\text{Al}_2\text{O}_3$ ) were reproducible to  $\pm 0.1\%$  on the basis of data from the National Institute of Standards and Technology (NIST).<sup>13</sup> The heat capacities of each polymer were determined in two different temperature ranges: range I 140–370 K for PDMSi, and for all others 140–420 K; range II from 360 K to just below the decomposition temperature. The latter measurements

Table I  
Temperature (K) at Which Weight Losses Occur on  
Heating at 10 K/min

polymer	first deviatn	wt loss		
		1%	5%	10%
poly(dimethylsilylene) (PDMSi)	523	533	594	615
poly(dipentylsilylene) (PDPSi)	493	518	545	562
poly(hexylsilylene) (PDHSi)	499	544	561	573
poly(ditetradecylsilylene) (PTDSi)	533	569	588	597

were carried out with the Perkin-Elmer DSC 7, and the heat capacity calculations were done with the commercial software supplied by Perkin-Elmer. All data were further corrected with sapphire heat capacities<sup>13</sup>.

Thermal stability of the samples was investigated with a TA 9900 thermal analyzer equipped with a 951 TG module. Helium was used as the purge gas. The heating rate was 10 K/min.

A Leitz polarizing microscope with a Mettler FP52 hot stage was used to detect the transition from the solid state to the melt for the various polysilylenes. All the samples were heated from 300 K to their decomposition temperature at 10 K/min and observed under a magnification of 400.

## Results

**Thermogravimetry.** The results of the thermogravimetry for the polysilylenes are summarized in Table I. A slight weight loss ( $\approx 2\%$ ) was observed in PDMSi between 300 and 380 K. Hence, the thermogravimetry was repeated for samples dried in a desiccator over  $P_2O_5$  for several days. PDMSi showed then a constant base line up to  $\approx 520$  K. Since PTDSi was shown earlier to have a transition at  $\approx 330$  K,<sup>11</sup> the analysis was carried out by first setting a controlled thermal history by heating the sample from  $\approx 350$ –420 K, followed by cooling at  $\approx 3$  K/min, from the mesophase to  $\approx 300$  K (the lowest possible temperature that could be achieved in the instrument). Thermogravimetry of the sample pretreated in such a way gave a horizontal base line without weight change up to the temperature of first decomposition ( $\approx 533$  K). All other samples yielded horizontal base lines up to the beginning of decomposition without special pretreatment. Since all the polysilylenes were stable to  $\approx 490$  K, the reported heat capacity measurements should be unaffected by decomposition.

**Differential Scanning Calorimetry of the Transitions.** (a) **Poly(dimethylsilylene) (PDMSi).** The Perkin-Elmer DSC 7 permitted evaluation of transitions down to  $\approx 210$  K. Figure 1 shows the DSC traces of PDMSi recorded for the sample dried for 48 h over  $P_2O_5$  (trace A) and a sample cooled at 10 K/min from 480 K and reheated at 10 K/min (trace B). Four distinct, but small, endotherms were observed in trace A. The first one is at  $\approx 235$  K and the remaining three appear at 300, 369, and 412 K. The high-temperature transition has a broad shoulder at  $\approx 430$  K. All heats of the endotherms are low when compared to typical enthalpies of fusion. The heats of transitions for the latter three endotherms are 64, 59, and 547 J/mol, respectively. Trace B showed only two endotherms, one at 239.6 K with a  $\Delta H = 162.7$  J/mol and one at 430.6 K with  $\Delta H = 560$  J/mol. The intermediate endotherms had disappeared on reheating. Heating of samples cooled from 480 K at 1 and 320 K/min caused no significant changes in either of the temperatures or heats of transition. Heating the sample to  $\approx 520$  K (beginning of decomposition) showed another small endotherm at 490 K ( $\Delta H$  approximately 400 J/mol). The endotherm at approximately 431 K agrees with the monoclinic-to-hexagonal transition, and the one at  $\approx 490$  K with some conformational and orientational disruption, reported

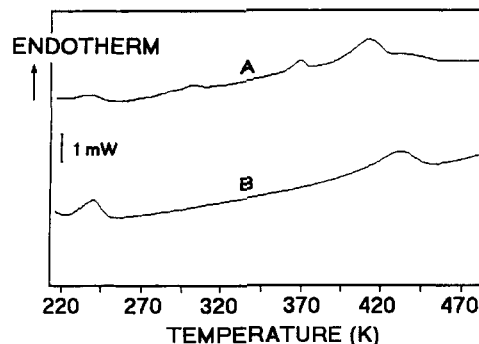


Figure 1. DSC traces of poly(dimethylsilylene) obtained at a heating rate of 10 K/min. Trace A is for a sample dried over  $P_2O_5$  for 48 h and trace B is for a sample cooled at 10 K/min from 480 K.

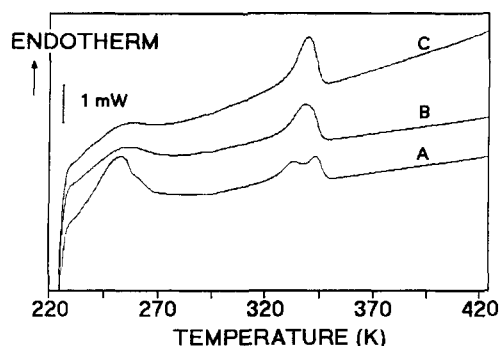


Figure 2. DSC traces of poly(dipentylsilylene) obtained at a heating rate of 10 K/min. Trace A is for the as-received sample, trace B is for a sample cooled at 10 K/min from 423 K, and trace C is for a sample cooled at 320 K/min from 423 K.

earlier.<sup>8</sup> The endotherms at 300 and  $\approx 369$  K in trace A were attributed to defect crystals.<sup>8</sup> Reorganization and crystal perfection on heating leads to better crystals, which on subsequent heating show a shift in endotherm to higher temperatures (trace B). The analysis of the heat capacity, below, suggests that none of the endotherms involves creation of major disorder in the crystals in agreement with the earlier work of ref 8.

(b) **Poly(dipentylsilylene) (PDPSi).** The DSC trace on heating the as-received sample of PDPSi is shown in Figure 2 (trace A). An initial transition with its onset being below the first temperature of measurement and a peak at 252 K with an approximate  $\Delta H$  of 2 kJ/mol is followed by a broad endotherm characterized by a double peak. It has a low  $\Delta H$  of 0.86 kJ/mol. The two peak temperatures are 332 and 342 K. Analysis of the thermal behavior beyond 423 K up to 508 K, just below the beginning of decomposition, indicated no further transition processes. A sample cooled at 10 K/min and reheated (trace B) showed a DSC curve similar to that observed in trace A, except that the higher temperature endotherm now appears as a single peak at 338 K with a total heat of transition of 1.3 kJ/mol. The peak temperature of the first peak was 253 K with a  $\Delta H$  of 1.1 kJ/mol. Samples cooled at 320 K/min from 423 K (trace C) showed the same thermal behavior as observed in trace B. Samples cooled at 5 and 1 K/min also showed the same transition behavior with a small change in the first peak (which could not be established well due to its beginning below the initial temperature of the experiment). The higher peak agreed with that reported earlier at 343 K.<sup>10</sup> The averages of four measurements are  $338.3 \pm 0.6$  K,  $1.41 \pm 0.12$  kJ/mol. The lower temperature peak will be shown from the discussion of the heat capacity data measurements not to be a hysteresis peak resulting from the glass transition,

Table II  
Various Thermodynamic Transitions in Polysilylenes<sup>a</sup>

polymer	$T_g$ , K	$\Delta C_p$ , J/(K mol)	$T_{(\text{onset})}$ , K	$T_d$ , K	$\Delta H_d$ , kJ/(mol)	$\Delta S_d$ , J/(K mol)	$T_i$ , K
PDMSi <sup>b</sup>			404.4	430.6 <sup>c</sup>	0.56 <sup>c</sup>	1.30 <sup>c</sup>	
PDPSi	227.4 (80)	47.7 (71.3) <sup>d</sup>	325.9	338.3	1.41	4.18 (12.7) <sup>d</sup>	518
PDHSi	220.5 (72)	37.9 (97.3) <sup>d</sup>	315.9	323.2	14.84	45.92 (75.3) <sup>d</sup>	533
PTDSi	(2 <sup>nd</sup> ) (8 <sup>th</sup> )	(148)	322.8	328.9	39.2	(119.2)	483

<sup>a</sup> The glass transition temperature and change in heat capacity at  $T_g$  were obtained from TA DSC used for heat capacity measurements from 160 K. The terms below  $T_g$  within parentheses represent the width of the glass transition temperature in kelvins.  $T_{(\text{onset})}$  is the extrapolation of the low-temperature side of the peak to the base line;  $T_d$  is the peak temperature; and  $T_i$  is the onset of isotropization detected by microscopy.

<sup>b</sup> PDMSi shows another transition at  $\approx 240$  K with a heat of transition of 0.16 kJ/mol and another one at  $\approx 490$  K with an approximate heat of transition of 0.4 kJ/mol. <sup>c</sup> This transition in PDMSi is a transition from one crystal form to another, probably without major increase in mobility. <sup>d</sup> Estimates for specific models and assumptions to yield 100% amorphous or crystalline data, see discussion.

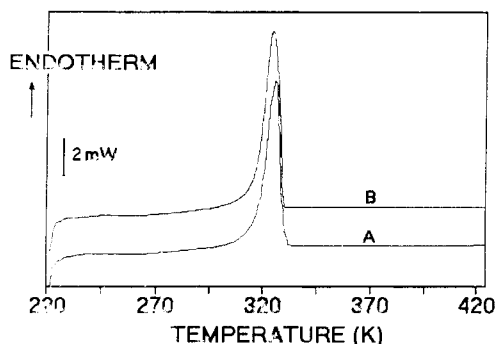


Figure 3. DSC traces of poly(dihexylsilylene) obtained at a heating rate of 10 K/min. Trace A is for the as-received sample and trace B is for a sample cooled at 320 K/min.

which occurs at 227.4 K ( $T_g$ ) with a  $\Delta C_p$  (change in heat capacity at  $T_g$ ) of 47.7 J/(K mol) (see Table II). A hysteresis peak should disappear when the sample is cooled at a rate equal to or higher than the rate at which it is heated. In PDPSi, the peak remains, even after the sample is cooled at 320 K/min and reheated at 10 K/min, thus giving reason to believe that this endotherm could be due to annealing during heating.

(c) **Poly(dihexylsilylene) (PDHSi).** Figure 3 shows the DSC traces of an as-received sample (trace A) and for a sample cooled at 320 K/min from 423 K, the condensation state of PDHSi (trace B). The onset of the transition for trace A, gained by extrapolating the peak to the base line, was at 316 K. The peak temperature was 324 K and a  $\Delta H$  of 14.6 kJ/mol was measured. For trace B the corresponding data are 316 K, 323 K, and 15.6 kJ/mol. Almost identical values were also obtained for samples cooled at 10, 5, and 1 K/min. The overall average of five measurements are  $315.9 \pm 0.74$  K,  $323.2 \pm 0.7$  K, and  $14.84 \pm 0.6$  kJ/mol. Heating the samples beyond 423 K, to just below the decomposition temperature, showed no further transitions. The peak at 323 K appeared at a slightly higher temperature than that reported by Schilling et al.<sup>10</sup> (314 K). Since the present analysis was done on an instrument limited to 210–220 K, the glass transition could only be detected through heat capacity measurements reported in the next section [ $T_g = 220.5$  K with a  $\Delta C_p$  of 37.9 J/(K mol)].

(d) **Poly(ditetradecylsilylene) (PTDSi).** Figure 4 shows the DSC traces of the as-received sample (trace A) and of a sample cooled at 10 K/min (trace B) from 423 K and heated at 10 K/min. Again, no glass transition is observed, as was the case for PDPSi and PDHSi. The broad endotherm, which appears as a broad doublet with some shoulders in the first run, changes in the subsequent scans, leaving a single peak with a broad onset. The peak temperature from an average of three measurements is at

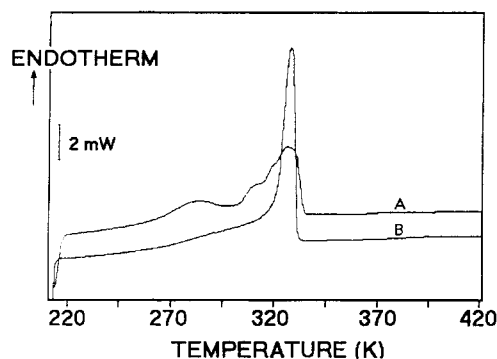


Figure 4. DSC traces of poly(ditetradecylsilylene) obtained at a heating rate of 10 K/min. Trace A is for as-received sample and trace B is for a sample cooled at 10 K/min from 423 K.

$328.9 \pm 0.3$  K with a heat of transition of  $39.2 \pm 0.35$  kJ/mol for all samples, irrespective of the different thermal histories of the samples. Again, no further transition was observed when the samples were heated to just below the decomposition temperature.

The transition data for all samples are summarized in Table II.

**Polarizing Microscopy.** In order to establish the nature of the transitions observed in the various polysilylenes, all samples were observed on a hot stage of a polarizing microscope while the temperature was increased from room temperature to just below decomposition. A sheared sample of PDMSi observed between crossed polarizer and analyzer showed no loss of birefringence up to  $\approx 560$  K, which is above the beginning of decomposition (see Table I). The sample remains thus a solid all through the experiment until it decomposes.

For PDPSi, PDHSi, and PTDSi, a melting transition was observed by microscopy. The edges of the birefringent objects become isotropic and start flowing at  $\approx 518$ , 533, and 483 K, respectively, for the three polysilylenes. Beyond this temperature a complete transition to the isotropic state was observed. From these results it is obvious that the change to the isotropic state occurs above the beginning or close to decomposition. These temperatures are above the transitions reported in the DSC described above, but qualitative analyses (DTA) through the decomposition region show no "melting endotherm"; i.e., fusion occurs with negligible latent heat. The onset temperatures for isotropization are also listed in Table II.

**Heat Capacities in the Solid and Liquid States by DSC. Experimental Procedures.** Heat capacities were measured for all the polysilylenes from 140 K to just below decomposition, to quantitatively analyze the nature of the observed transitions. For all the samples an average of three to five measurements was used. In each case the

samples were cooled with liquid nitrogen at an uncontrolled rate and sufficient time was given for equilibrium to be established before the heating was recorded. Discarding the first few data points, the solid-state heat capacity of the polysilylenes, determined in the temperature range 160–190 K for PDMSi and for the rest 160–200 K, can be described by the equations

## PDMSi

$$C_p = 31.13 + 0.2141T (\pm 0.16\%) \quad [\text{J}/(\text{K mol})] \quad (1)$$

## PDPSi

$$C_p = 28.89 + 1.1859T - 0.001182T^2 (\pm 0.12\%) \quad [\text{J}/(\text{K mol})] \quad (2)$$

## PDHSi

$$C_p = 70.47 + 0.8128T - 0.000291T^2 (\pm 0.25\%) \quad [\text{J}/(\text{K mol})] \quad (3)$$

## PTDSi

$$C_p = 45.86 + 2.3449T - 0.001279T^2 (\pm 0.4\%) \quad [\text{J}/(\text{K mol})] \quad (4)$$

From 200 to 490 K the experimental heat capacities for PDMSi (from an average of three runs) were interpolated by using a spline function technique and are shown in Table III. The heat capacities of the data are described to a precision of  $\pm 0.5\%$ . The heat capacities of the other three polysilylenes in the transition range were similarly smoothed and are also shown in Table III. Beyond the transition region the following equations hold:

## PDPSi (360–490 K)

$$C_p = -186.85 + 2.4320T - 0.002398T^2 (\pm 0.05\%) \quad [\text{J}/(\text{K mol})] \quad (5)$$

## PDHSi (360–500 K)

$$C_p = 93.51 - 4.4857T + 0.011893T^2 (\pm 0.13\%) \quad [\text{J}/(\text{K mol})] \quad (6)$$

## PTDSi (360–500 K)

$$C_p = -1.163 + 3.4362T - 0.002516T^2 (\pm 0.2\%) \quad [\text{J}/(\text{K mol})] \quad (7)$$

**Computation of the Heat Capacity of the Solids.** Experimental heat capacities for the solid state were available from 160 K to the glass transition temperatures of PDPSi, PDHSi, and PTDSi, and to 190 K (below the first transition) for PDMSi. By use of the well-established ATHAS computation scheme described in several publications,<sup>14</sup> heat capacities were calculated for the solids based on approximate vibrational spectra. For this purpose the vibrational spectrum was separated into group and skeletal parts as listed in Table IV. The group vibrations for the  $\text{CH}_3$  group in PDMSi were obtained from the IR and Raman data available.<sup>15</sup> For the various poly(di-*n*-alkylsilylenes), the group vibrations of the  $\text{CH}_3$  and the  $\text{CH}_2$  group were retrieved from the IR spectra of

**Table III**  
Experimental Heat Capacity of Polysilylenes

T, K	heat capacity, J/(K mol)			
	PDMSi	PDPSi	PDHSi	PTSi
200	73.94			
210	76.26	227.5	255.5	485.3
220	79.54	239.3	217.6	509.2
230	83.74	256.4	295.1	535.2
240	86.95	286.9	322.6	565.0
250	81.79	319.9	333.2	601.9
260	81.80	326.1	333.1	652.1
270	82.74	313.2	344.8	705.8
280	84.37	313.3	362.8	783.1
290	85.56	318.8	385.3	871.3
300	86.86	326.6	420.6	963.8
310	89.01	335.6	500.7	1058.0
320	91.20	348.1	1295.2	1248.0
330	93.49	375.0	508.6	3350.0
340	95.91	446.1	409.0	895.0
350	98.40	354.7	413.8	886.0
360	101.0			
370	103.9			
380	106.9			
390	110.4			
400	114.6			
410	119.8			
420	126.5			
430	133.3			
440	129.6			
450	123.5			
460	123.9			
470	126.8			
480	130.2			
490	134.1			

**Table IV**  
Number of Vibrational Modes Used as Group Vibrations

approximate mode	PDMSi	PDPSi	PDHSi	PTDSi
(a) $\text{CH}_3$ asym stretch	4	4	4	4
$\text{CH}_3$ sym stretch	2	2	2	2
$\text{CH}_3$ asym bend	2	2	2	2
$\text{CH}_3$ sym bend	2	2	2	2
$\text{CH}_3$ rock	4	4	4	4
(b) $\text{CH}_2$ asym stretch		8	10	26
$\text{CH}_2$ sym stretch		8	10	26
$\text{CH}_2$ bend		8	10	26
$\text{CH}_2$ wag		8	10	26
$\text{CH}_2$ twist		8	10	26
$\text{CH}_2$ rock		8	10	26
C–C stretch		8	10	26
(c) Si– $\text{CH}_3$ asym stretch	1			
Si– $\text{CH}_3$ sym stretch	1			
Si– $\text{CH}_2$ asym stretch		1	1	1
Si– $\text{CH}_2$ sym stretch		1	1	1
(d) Si–Si asym stretch	0.5	0.5	0.5	0.5
Si–Si sym stretch	0.5	0.5	0.5	0.5
total group vibratnl modes	19	75	89	201
skeletal vibratnl modes	8	24	28	60
total vibratnl modes	27	99	117	261

the poly(di-*n*-alkylsilylenes) described by Rabolt<sup>3</sup> and normal-mode calculations of polypropylene<sup>16</sup> (for the  $\text{CH}_3$  vibrational modes). The Si–Si backbone asymmetric and symmetric stretching modes appear at 647.5–719.4 and 532.4 K, respectively.<sup>17</sup> The group vibrations, expressed in kelvin ( $1 \text{ K} = 0.695 \text{ cm}^{-1} = 2.08 \times 10^{10} \text{ Hz}$ ;  $h\nu/k = \theta$ ), are listed in Table V. Subtracting the group vibrational contribution to the heat capacity from the experimental data and fitting the resulting skeletal heat capacity to a one-dimensional Debye function<sup>14</sup> gave values of  $\theta_1 = 342 \pm 6 \text{ K}$  for PDMSi (from 160 to 190 K),  $320 \pm 25 \text{ K}$  for PDPSi (from 160 to 200 K),  $412 \pm 16 \text{ K}$  for PDHSi (from 160 to 200 K), and  $593 \pm 2 \text{ K}$  for PTDSi (from 160 to 200 K). These  $\theta$  values largely represent the intramolecular contribution to the skeletal heat capacity. Since no

Table V  
Group Vibration Frequencies in Kelvin ( $h\nu/k$ )

approx vibrational mode		N	frequency, K
(a) CH <sub>3</sub> poly(dimethylsilylene) <sup>a</sup>	CH <sub>3</sub> asym stretch	2	4259
	CH <sub>3</sub> sym stretch	1	4180
	CH <sub>3</sub> asym bend	2	2043
	CH <sub>3</sub> sym stretch	1	1813
	CH <sub>3</sub> rock	2	1273
(b) CH <sub>3</sub> poly(di- <i>n</i> -alkylsilylenes) <sup>b</sup>	CH <sub>3</sub> asym stretch	2	4260.8
	CH <sub>3</sub> sym stretch	1	4130.8
	CH <sub>3</sub> asym bend	1	2107
	CH <sub>3</sub> asym bend	1	2101
	CH <sub>3</sub> sym bend	0.25	1987
		0.38	1973–1987
		0.37	1973
	CH <sub>3</sub> rock (CH <sub>2</sub> wag)	0.55	1453–1521
		0.45	1453
	CH <sub>3</sub> rock	0.65	1361–1393
(c) CH <sub>2</sub> poly(di- <i>n</i> -alkylsilylenes) <sup>c</sup>	CH <sub>2</sub> asym stretch	2	4207.1
	CH <sub>2</sub> sym stretch	2	4106
	CH <sub>2</sub> bend	2	2116.5
	CH <sub>2</sub> wag	2	1774
	CH <sub>2</sub> twist	2	1690.6
	CH <sub>2</sub> rock	2	1046
(d) C–C chain stretch in side chains <sup>c</sup>	C–C stretch	0.5	1597.1
	C–C stretch	0.5	1405.7
(d) Si–CH <sub>2</sub> poly(di- <i>n</i> -alkylsilylenes) <sup>c</sup>	Si–CH <sub>2</sub> asym stretch	1	1158
	Si–CH <sub>2</sub> sym stretch	1	1022
(e) Si–Si backbone <sup>d</sup>	Si–Si asym stretch	0.5	647.5–719.4
	Si–Si sym. stretch	0.5	532.4

<sup>a</sup> CH<sub>3</sub> group frequencies obtained from IR and Raman spectra.<sup>15</sup>

<sup>b</sup> Frequency ranges from normal-mode calculation of polypropylene.<sup>16</sup>

<sup>c</sup> Frequency ranges from IR of poly(di-*n*-alkylsilylenes).<sup>3</sup> <sup>d</sup> Frequency ranges from Raman data.<sup>17</sup>

experimental heat capacities are available below 160 K, an estimated  $\theta_3$  of 67.55 K [the same as that of poly(dimethylsiloxane)]<sup>18</sup> was used as a guess to represent the intermolecular contribution to the skeletal heat capacity. All  $C_p$  to  $C_v$  conversions and vice versa were made with the modified Nernst–Lindemann equation using the universal value of  $A_0 = 0.0039$  (K mol)/J.<sup>19</sup> For these conversions at least an approximate melting temperature is needed. Based on information from polarizing microscopy, values of 520, 530, and 480 K were used as estimates of the equilibrium melting temperatures for PDPSi, PDHSi, and PTDSi, respectively. For PDMSi a guess of 600 K was made. Heat capacities were finally computed for the solids by using the above derived  $\theta_1$  and  $\theta_3$  to represent the skeletal vibrations and combining their contributions with the group vibrational contributions as outlined in Tables IV and V.

The low-temperature experimental heat capacity agrees with the calculated data over the range of measurement with an average and root-mean-square error of  $-0.16 \pm 0.45\%$  for PDMSi,  $0.88 \pm 1.6\%$  for PDPSi,  $0.5 \pm 0.94\%$  for PDHSi, and  $2.0 \pm 0.16\%$  for PTDSi. The calculated solid heat capacities are plotted in Figures 5–8, along with the experimental heat capacity and, where needed, the liquid heat capacities determined through an addition scheme described below. Readers interested in tables of the computed heat capacities from our data bank of over 150 polymers may request these from us.

**Addition Scheme for Liquid Heat Capacities.** The comparison of the phase behavior via thermal analysis

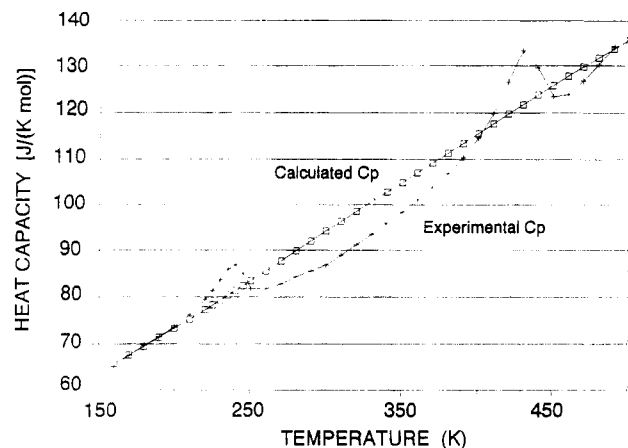


Figure 5. Heat capacity of poly(dimethylsilylene).  $\square$ , vibration-only  $C_p$  calculated by using the ATHAS computation scheme; +, experimental  $C_p$ .

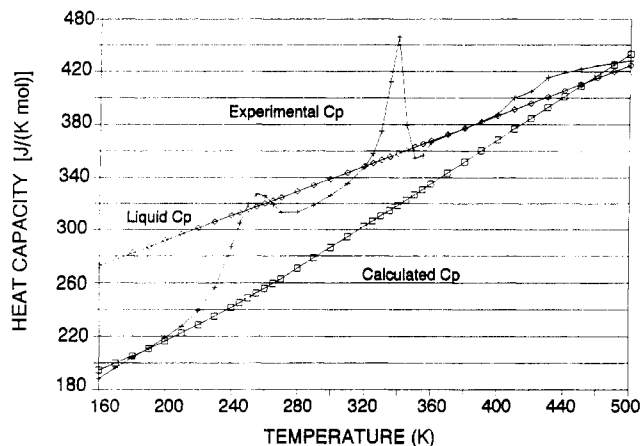


Figure 6. Heat capacity of poly(dipentylsilylene).  $\square$ , vibration-only  $C_p$  computed by using the ATHAS computation scheme; +, experimental  $C_p$ ;  $\diamond$ , liquid  $C_p$  obtained by use of the empirical addition scheme considering all groups to be mobile.

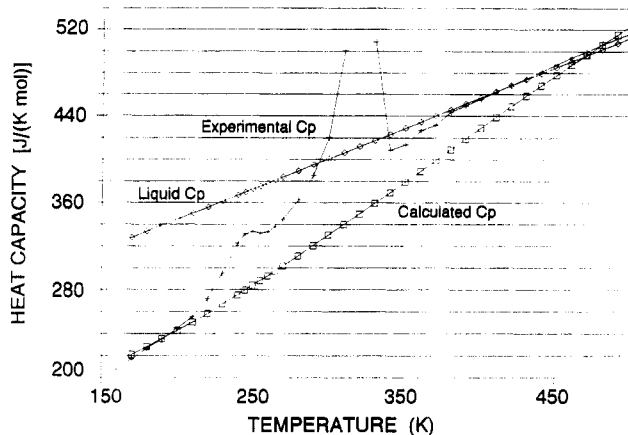


Figure 7. Heat capacity of poly(dihexylsilylene).  $\square$ , vibration-only  $C_p$  computed by using the ATHAS computation scheme; +, experimental  $C_p$ ;  $\diamond$ , liquid  $C_p$  obtained by use of the empirical addition scheme considering all groups to be mobile.

and polarizing microscopy has revealed that beyond the order-disorder transition the polysilylenes with  $C_5$ ,  $C_6$ , and  $C_{14}$  side chains transform into an isotropic melt through a process that has no major endotherm. For PDPSi and PDHSi the observed isotropization temperatures of 518 and 533 K were close to the beginning of decomposition so that it was not possible to measure the melt heat capacities. For PTDSi the liquid heat capacity was available only over the range 480–510 K. Hence, to

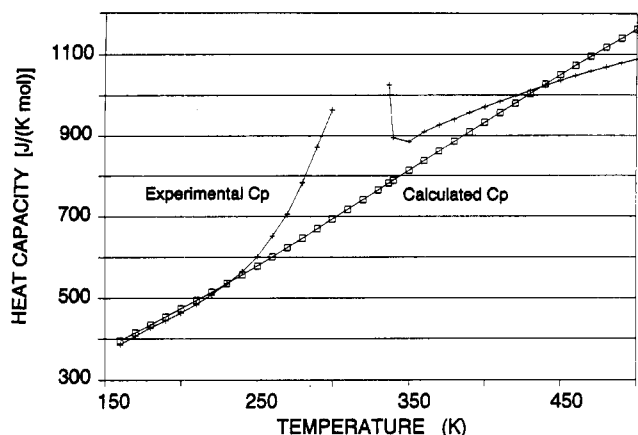


Figure 8. Heat capacity of poly(ditetradecylsilylene).  $\square$ , vibration-only  $C_p$  computed by using the ATHAS computation scheme; +, experimental  $C_p$ .

fully analyze the glass transition and the disordering transition, an empirical addition scheme was used for the liquid heat capacities, as it was developed earlier for other linear macromolecules.<sup>20</sup> The contribution of the  $[\text{Si}(\text{CH}_3)_2]_n$  group was determined by subtracting the O group contribution from the experimental liquid heat capacity of poly(dimethylsiloxane). The methylene group contributions were used as found for the liquid heat capacity of polyethylene.<sup>21</sup> The heat capacity obtained by adding the contributions of the various groups for PDPSi and PDHSi are shown in Figures 6 and 7. No data for PDMSi liquid are shown in Figure 5 since no glass transition or melt was observed for this polymer. For PTDSi a sufficient range of measurement is available for the mobile phase.

## Discussion

**Heat Capacities.** The heat capacities of the solid, calculated from 0.1 to 1000 K by fitting the experimental  $C_p$  over a limited temperature range of 160–200 K and using the data of Tables IV and V, and the liquid heat capacities obtained through an empirical addition scheme enable us to draw better base lines for the DSC curves. From  $\approx 50$  K to the glass transition the heat capacities of the solids are largely independent of the state of order of the polymer and the differences between the heat capacities of amorphous, semicrystalline, and crystalline samples are small. Heat capacities of the solid can usually be computed in this temperature range based purely on vibrational contributions. Changes in the vibrational spectrum due to different degrees of order occur only at low frequency and affect the heat capacity below 50 K.

As expected, the Tarasov equation used to represent the skeletal vibration worked well for PDMSi in which the molecule is still quite linear and the mass distribution and force constants do not vary significantly along the chain. A similar agreement was found for polypropylene.<sup>16</sup> In the cases of PDPSi, PDHSi, and PTDSi with two symmetrical  $\text{C}_5$ ,  $\text{C}_8$ , and  $\text{C}_{14}$  side chains, we represent the side chains as part of a skeletal backbone (see Table IV). This is a choice justified by the agreement between calculated and experimental heat capacities within the customary experimental uncertainty of about  $\pm 3\%$ . It was also found recently that paraffins from about six to seven carbon atoms in length up to polyethylene follow a continuous change in  $\theta$  temperature and have their heat capacity well represented by a Tarasov function<sup>22</sup> and a similar table of group vibrations.

The progression of  $\theta_1$  temperatures with side-chain length starts with a relatively low value of 342 K for PDMSi,

characteristic of the backbone chain, and increases to 593 K for PTDSi, a value not much different from polyethylene and the paraffins (519 K).

**Glass Transition.** The glass transition of the polysilylenes can be discussed along two routes. The first makes use of standard interpretation of the heat capacity of the solid and liquid. The second starts from the assumption that a silicon backbone atom substituted with two alkane chains is sterically hindered to such a degree that the Si and four  $\text{CH}_2$  groups (two for each side chain) remain a grouping (bead) of fixed conformation up to  $\approx 500$  K, irrespective of its physical state. A discussion of the glass transition, and later on the disordering transition, is then concerned with the remaining shortened side chains only.

For PDMSi no clear  $T_g$  was observed in Figure 1. Assuming the upturn of  $C_p$  at  $\approx 180$  K to be connected with a glass transition would lead, using the addition scheme heat capacity of the liquid  $[\text{Si}(\text{CH}_3)_2\text{O} - \text{minus O-}]$ , to a  $\Delta C_p$  of only  $\approx 5$  J/(K mol). From a comparison with all other flexible linear macromolecules this accounts for only 0.5 chain atom. Since after the maximum in  $C_p$  a broad, shallow minimum follows with a heat capacity less than that of the computed rigid solid (see Figure 5), this interpretation remains uncertain. More likely, PDMSi is highly crystalline<sup>8</sup> or contains rigid amorphous polymer and the fluctuation of the measured heat capacity about the computed "vibration-only" heat capacity is linked to minor changes in crystal packing or relaxation of strained amorphous. The heat capacity deviations do not exceed 10%, even at the maxima and minima. This is too close to the experimental uncertainty to further speculate about the origin. Figure 5 reveals that the endotherms and exotherms added over the whole temperature range of measurement average close to zero.

More information can be gained for PDPSi and PDHSi. From Figures 6 and 7 glass transitions are obvious at 227.4 and 220.5 K, respectively (see Table II). A glass transition for PDPSi at 233 K was reported earlier,<sup>10</sup> while none was detected for PDHSi. The experimental  $\Delta C_p$ 's listed in Table II are less than those estimated from the liquid heat capacity at the same temperature. The latter would correspond to a completely amorphous sample (values in parentheses in Table II). Using the expression

$$\text{crystallinity} = 1 - [\Delta C_p(\text{semicryst}) / \Delta C_p(\text{amorph})] \quad (8)$$

one can determine crystallinities of 33% and 61% for the PDPSi and PDHSi, respectively. These values will be further compared to information gained from the heats disordering, below.

The second analysis route requires an estimate of the heat capacity of a mobile  $\text{CH}_2$  group above the glass transition. Since paraffins and polyethylene have the same  $\text{CH}_2$  heat capacity contributions, both, in the solid and liquid states,<sup>22</sup> one can estimate that at  $\approx 225$  K, the  $T_g$  of PDPSi and PDHSi, the increase in heat capacity at  $T_g$  is  $\Delta C_p = 10.7 \text{ J}/[\text{K}(\text{mol of } \text{CH}_2)]$ .<sup>21</sup> For PDHSi one calculates from the data in Table II that four to five  $\text{CH}_2$  groups behave as if they were glassy. For PDHSi one finds three to four glassy  $\text{CH}_2$  groups that become mobile. These data must be compared to the gain in mobility in the crystalline portion of the molecules at the disordering transitions,  $T_d$ , to be discussed below.

The data on PTDSi show, again, no obvious glass transition in Figures 4 and 8. One notices, however, that after  $T_d$  the heat capacity joins smoothly that of the liquid state above 480 K, while below  $T_d$ ,  $C_p$  is purely vibrational. One must assume, thus, that the glass transition and the

disordering transition occur in the same temperature region. Polyethylene has a  $T_g$  of 237 K,<sup>23</sup> sufficiently close to the beginning of disordering in PTDSi to make this assumption reasonable. From eqs 7 and 4 one computes a  $\Delta C_p$  of 148 J/(K mol) at 250 K, while the addition scheme heat capacity of the liquid would lead to a  $\Delta C_p$  of as much as 250 J/(K mol) (24 mobile  $\text{CH}_2$  groups). Curve B in Figure 4 is thus perhaps best interpreted as showing a glass transition broadened and probably shifted to higher temperature due to side-chain crystallinity. It begins at  $\approx 240$  K and reaches to the onset of disordering at 323 K.

**Order-Disorder Transition.** The optical microscopy and thermogravimetry revealed that PDMSi showed no fusion before decomposition and the other polysilylenes started to become isotropic in a temperature region that does not have a prominent endotherm and is close to decomposition. All of the observed larger endotherms must thus be disordering transitions. From the general discussion of conformational disorder of molecules with paraffins side chains one expects condic crystals (crystals with conformational disorder).<sup>24,25</sup> The type of condic crystal of particular interest is that of a flexible chain attached to a backbone of fixed conformation, as described in section 5.3.4 of ref 24. After a certain length of the flexible chain is reached, well-defined disordering transitions are observed involving mainly the side chain. The overall crystal integrity is in these cases not disturbed due to the unchanged backbone conformation. Other examples of such substrates for attachment of disordered paraffinic chains are silicate layer crystals and poly(L-glutamate) and poly(1,4-phenylene terephthalate) backbones.<sup>24</sup> A three-dimensional substrate of sufficient rigidity to support disordered, mobile chains can also be provided by an anionic crystal, as for example in tetraalkylammonium salts,<sup>26</sup> of which an extended series is presently under investigation in our laboratory.

The first of the homologous series of polysilylenes, PDMSi, shows only small "transitions". An entropy of transition of 1.3 J/(K mol), as listed in Table II, could account for no more than 10% of a typical entropy observed on introduction of 1 mol of conformational disorder. The average entropy increase per mole of conformational motion gained has been estimated by analysis of melting and disordering transitions to be 7–12 J/(K mol).<sup>27</sup> One must conclude that PDMSi is highly crystalline or has a large rigid amorphous fraction and shows only minor changes in crystal packing or relaxation of strained amorphous.

The next two polysilylenes, PDPSi and PDHSi, have similar transitions (Figures 2, 3, 6, and 7), but differ in their entropies of disordering (Table II). The transitions at 338 and 323 K were identified earlier as involving disordering of the side chains.<sup>11</sup> Through the study of silicon chemical shift and  $^{13}\text{C}$  spin-lattice relaxation data<sup>10</sup> it was shown that above the disordering transition the average chain conformation of the silicon backbone and the motion of the silicon nuclei are the same in PDPSi, PDPSi, and PDHSi. In all cases there is rapid motional averaging.

By use of the crystallinity values derived from the glass transition discussion,  $\Delta S_d$  for completely ordered crystals becomes 12.7 and 75.3 J/(K mol), respectively, for PDPSi and PDHSi, accounting for 1–2 and 6–10 conformations gaining full disorder.

By the second route of analysis of the glass transition above, there are four to five disordered  $\text{CH}_2$  groups in PDPSi and the disordering transition at 338 K adds less than one more. Each side chain must thus have about two

C atoms that are not gaining disorder over the whole range of temperature. Additional evidence on the limited mobility of the inner portion of the side chain can also be derived from the  $^1\text{H}$  and  $^{13}\text{C}$  NMR spectra, as is shown in the next section. Thus, if one considers two carbons in each side chain as possessing fixed conformations (i.e., not contributing to the glass and disordering transition), one must, as concluded from the PDPSi data, account for a total of eight remaining  $\text{CH}_2$  units in the two side chains of PDHSi. In the present analysis we were able to estimate that about four are accounted for by the glass transition and the other four by the disordering transition. These "side-chain crystallinities" of 17% and 50% for PDPSi and PDHSi, respectively, must be compared to the "overall crystallinities" computed from eq 8.

The PTDSi of Figures 4 and 8 show a much larger disordering transition. Using the typical entropy change of 7–12 J/(K mol) per conformational degree of freedom, the data in Table II can account for 10–17  $\text{CH}_2$  groups disordering at 329 K. A possible glass transition was shown above to be possible in the same temperature range. By use of the  $\Delta C_p$  of Table II, this can account easily for the remaining  $\text{CH}_2$  groups. Within the rather coarse estimates of this analysis it seems, thus, that the broadness of the disordering peak accounts, indeed, for a glass transition. Additional information is needed for a proper apportionment of the base line between the glass transition and the disordering transition. The data in Table II give both maximal glass transition and maximal heat of disordering.

It was suggested by Weber et al.<sup>28</sup> at about the same time that above the disordering transition PDHSi exists in the liquid-crystalline state. It was noted that the polymer shows hexagonal columnar symmetry and the silicon backbone was suggested to be all-gauche. The mobility detected by NMR makes the all-gauche assignment unlikely, and the suggestion of these polymers being liquid crystals above their disordering transition needs some additional comment. The difference between condic crystals and liquid crystals was outlined in refs 24 and 25. The condic crystal should have molecular positional and orientational order. It was shown on several examples that, if the chemical structure allows, liquid crystals show close to the same conformational disorder as the melt.<sup>29–32</sup> For small molecules the transition of a liquid crystal to the isotropic state is usually an endothermic, reversible, first-order transition with a small orientational entropy increase.<sup>25</sup> Macroscopic liquid crystals that emulate low molecular mass liquid crystals behave similarly.<sup>25</sup> They normally consist of flexible chain segments separating rigid mesogens. In the present case there are no rigid mesogens, making the assignment of the samples as liquid crystals problematic. A macromolecular crystal has, because of its large size, practically no positional and orientational entropy of fusion.<sup>27</sup> In the present case, the side-chain disorder at the disordering transition is already almost that of the isotropic melt. This leaves as remaining potential disorder that of the backbone,  $\approx 9$  J/(K mol).<sup>27</sup> Such transition entropy is, however, not observed.

The NMR evidence<sup>10,11</sup> indicates large amplitude motion in the high-temperature phase II, but not enough to produce an isotropic state. Neither an all-trans nor an all-gauche state is thus likely. The conformational mobility of the backbone must be, however, such that the overall orientational and positional order is kept.

The remaining question concerns the "transitionless" isotropization observed by microscopy for PDPSi, PDHSi, and PTDSi. For PDPSi, and to a lesser degree of PDHSi, the shallow endotherm above the disordering transition



may signal further disordering. Overall, however, there is considerable evidence that condic crystals can gradually gain mobility to become isotropic. Other examples that were analyzed in our laboratory included poly(diethylsiloxane),<sup>33</sup> poly(oxybenzoate), and poly(oxynaphthoate).<sup>34</sup> Similarly a number of polyphosphazenes fall into this category.<sup>24</sup> In all these materials the condic crystals seem to become isotropic without a sharp transition. Naturally, a condic crystal that changes gradually to the isotropic state may during this change also become similar to the liquid-crystalline state. The major difference remains the nonexistence of a permanent, rigid mesogen. Close to the disordering transition, the backbone chains remain extended to the crystal dimension. Close to the isotropization temperature, the extended segments are too short to suggest a liquid-crystalline state (variable mesogens). This property of some condic crystals has not seen much experimental or theoretical attention.

**NMR Evidence of Side-Chain Motion in PDPSi and PDHSi.** It was shown by Schilling et al.<sup>10</sup> by measurement of the <sup>13</sup>C spin-lattice relaxation times,  $T_1$ , that, except for the CH<sub>3</sub> rotation, the correlation times of all the side-chain <sup>13</sup>C nuclei decrease from ca. 100 ns for PDPSi and ca. 1 μs for PDHSi in the room-temperature phase I to ca. 1 ns for both polymers in their respective high-temperature phases II. The <sup>29</sup>Si nuclei of both polymers in phase II have also much shorter  $T_1$ 's than in phase I, reflecting the increase of mobility in the backbone which was attributed to conformational averaging.<sup>10</sup> On the basis of our analysis of the DSC data it seemed probable that in phase II (1) the increase of mobility in the inner methylenes of the side chains is due to the motion in the silicon backbone, i.e., they remain rigid by themselves, (2) while for outer CH<sub>2</sub>'s the motion is a composite of the Si backbone motion and the local segmental motion, i.e., there exists additional conformational motion and disorder about C-C bonds, measurable by DSC.

To see if these conclusions from DSC agree with the NMR results in the literature it is necessary to separate the backbone motion from the overall motion. The motion of the backbone contributes little to the entropy at the transition. The motion in the side chain is responsible for most of the entropy change during the order-disorder transitions. Using the data by Schilling et al.,<sup>10</sup> we were able to separate the two types of motion in the side chain employing the following considerations for the  $T_1$ 's of the side chain (<sup>13</sup>C NMR). It was indicated by Lyrerla<sup>35</sup> that for large molecules with a number of reorientational modes the relaxation data can be analyzed semiquantitatively to obtain effective correlation times  $\tau^{\text{eff}}$  for each carbon via

$$\frac{1}{nT_{1C}} = \frac{\gamma_C^2 \gamma_H^2 \hbar^2}{40 \pi^2 r^6} \left[ \frac{\tau}{1 + (\omega_H - \omega_C)\tau^2} + \frac{3\tau}{1 + \omega_C^2 \tau^2} + \frac{6\tau}{1 + (\omega_H + \omega_C)^2 \tau^2} \right] \quad (9)$$

where  $\gamma_H$  and  $\gamma_C$  are the magnetogyric ratios of the <sup>1</sup>H and <sup>13</sup>C nuclei, respectively. The constants,  $\omega_H$  and  $\omega_C$  are the resonant frequencies in radians/s for <sup>1</sup>H and <sup>13</sup>C, respectively ( $2\pi \times 200$  MHz and  $2\pi \times 50.3$  MHz in ref 10). The distance between the interacting nuclei <sup>13</sup>C and <sup>1</sup>H,  $r$ , can be taken as 0.109 nm in methylene and methyl groups. The number  $n$  is the number of the protons attached to the carbon; for a methylene group  $n = 2$  and for a methyl group  $n = 3$ . The correlation time  $\tau$  is then determined by the measured  $T_1$ . The  $T_1$  given by eq 9 shows a minimum at  $\omega_C \tau = 0.793$ , or  $\tau = 2.52$  ns. The temperature dependence of  $T_1$  for each carbon and the progressive

**Table VI**  
<sup>13</sup>C Spin-Lattice Relaxation Times<sup>10</sup> and Effective Correlation Times<sup>a</sup> (in ps, as Calculated) for the Side-Chain Carbons in Poly(di-*n*-alkylsilylene)<sup>b</sup>

polymer	$\tau^{\text{eff}}(T_1)$ , s					
	C1	C2	C3	C4	C5	C6
PDBSi	133.0 (0.18)	103.0 (0.23)	53.18 (0.44)	11.10 (1.4)		
PDPSi	151.0 (0.16)	125.7 (0.19)	65.15 (0.36)	32.41 (0.72)	11.95 (1.3)	
PDHSi	161.7 (0.15)	133.03 (0.18)	81.19 (0.29)	42.48 (0.55)	24.81 (0.94)	7.060 (2.2)

<sup>a</sup> Values in parentheses, in picoseconds (as newly calculated).

<sup>b</sup> Computed with the data of ref 10, C 1 is the carbon atom attached to the Si.

**Table VII**  
Differential Rates  $1/\tau(l,m)$ <sup>a</sup> Corresponding to Differences in Conformational Mobilities of the Side-Chain Carbons in PDBSi, PDPSi, and PDHSi in Phase II

polymer	$1/\tau(1,2)$	$1/\tau(2,3)$	$1/\tau(3,4)$	$1/\tau(4,5)$	$1/\tau(5,6)$
PDBSi	0.219	0.910	7.13		
PDPSi	0.133	0.740	1.55	5.28	
PDHSi	0.133	0.479	1.12	1.68	10.1

<sup>a</sup> In  $10^{10}$  s<sup>-1</sup>.

increase of  $T_1$  from the carbon atom next to the Si to the chain end in phase II of both polymers suggests that the correlation times are at the short-time side of the  $T_1$  minimum. The measured  $T_1$  data<sup>10</sup> and the calculated effective correlation times,  $\tau^{\text{eff}}$ , are given in Table VI for the side chains for PDPSi and PDHSi in phase II. The values of PDBSi are also listed for comparison.

Next, we separate the motion of the C-H vector in the side chains in terms of motion in the side chains (considered as a rigid rod) caused by the Si motion with and average rate  $\tau_o^{-1}$  and an internal conformational motion about the individual C-C bonds in the side chains with rate  $\tau_i^{-1}$ . The expression for the rate of motions of the  $j$ th carbon in the side chain,  $(\tau^j)^{-1}$ , is then the sum of the two rates:<sup>35</sup>

$$\frac{1}{\tau^j} = \frac{1}{\tau_o^j} + \frac{1}{\tau_i^j} \quad (10)$$

The differential rate between the  $l$ th and  $m$ th carbons is

$$[\tau(l,m)]^{-1} = \frac{1}{\tau^l} - \frac{1}{\tau^m} \quad (11)$$

Substituting eq 10 into eq 11, and realizing that  $1/\tau_o^l = 1/\tau_o^m$ , eq 11 becomes

$$[\tau(l,m)]^{-1} = \frac{1}{\tau_i^l} - \frac{1}{\tau_i^m} \quad (12)$$

The quantity  $1/\tau(l,m)$  should involve only internal correlation times and represents the difference in rates of the conformational motion, between the  $l$ th and  $m$ th carbons. By use of the results given in Table VI, the differential rates of internal motion in PDBSi, PDPSi, and PDHSi were calculated as shown in Table VII.

The small differential rates in the interior bonds indicate slow conformational motions, very much in line with the calorimetric result that two of the CH<sub>2</sub> remain conformationally immobile.

It should be noted that the trends toward decreased conformational mobility near the point of attachment of a side chain is also observed in the cations of tetra-*n*-alkylammonium halides, which have structures similar to the junction regions of the polymers under consideration.<sup>36</sup> Results for *n*-hexyltrimethylammonium bromides also



reveal a similar trend of decreased segmental mobility at the polar end of the molecule.<sup>37</sup> Another example of the decrease of segmental motion of an alkyl side chains is that of poly(*n*-butyl methacrylate) in solution.<sup>38</sup> The semi-quantitative treatment of the effective correlation times of carbons in the butyl side group based on the <sup>13</sup>C T<sub>1</sub> data shows results remarkably similar to those of PDPSi.

### Conclusions

The thermal analyses of the polysilylenes reveal, in accord with X-ray data,<sup>11</sup> the existence of condensation crystals for PDPSi, PDHSi, and PTDSi. The side chains of these three polymers are only partially crystalline. Approximately two C atoms of each side chain seem not to contribute to either the glass transition or the disordering transition. Of the remaining CH<sub>2</sub> groups some show a glass transition, and the others a disordering transition. The isotropization observed by optical microscopy shows no major thermal effect. The first member of the series, PDMSi, shows only minor packing changes and decomposes before fusion.

**Acknowledgment.** This work was supported by the Division of Materials Research, National Science Foundation, Polymers Program, Grant DMR 8818412 and the Division of Materials Sciences, Office of Basic Energy Sciences, U.S. Department of Energy, under Contract DE-AC05-84OR21400 with Martin Marietta Energy Systems, Inc. We also thank Dr. R. D. Miller of IBM, San Jose, for providing the samples of PDPSi, PDHSi, and PTDSi.

### References and Notes

- (1) Kuzmany, H.; Rabolt, J. F.; Farmer, B. L.; Miller, R. D. *J. Chem. Phys.* **1986**, *85*, 7413.
- (2) Harrah, L. A.; Zeigler, J. M. *Macromolecules* **1987**, *20*, 601.
- (3) Rabolt, J. F.; Hofer, D.; Miller, R. D.; Fickes, G. N. *Macromolecules* **1986**, *19*, 611.
- (4) Hallmark, V. M.; Sooriyakumaran, R.; Miller, R. D.; Rabolt, J. F. *J. Chem. Phys.* **1989**, *90*, 2486.
- (5) Lovinger, A. J.; Schilling, F. C.; Bovey, F. A.; Zeigler, J. M. *Macromolecules* **1986**, *19*, 2657.
- (6) Schilling, F. C.; Bovey, F. A.; Lovinger, A. J.; Zeigler, J. M. *Macromolecules* **1986**, *19*, 2660.
- (7) Grobby, G. C.; Fleming, W. W.; Sooriyakumaran, R.; Miller, R. D. *J. Am. Chem. Soc.* **1986**, *108*, 5624.
- (8) Lovinger, A. J.; Davis, D. D.; Schilling, F. C.; Padden, F. J., Jr.; Bovey, F. A.; Zeigler, J. M. *Polym. Prepr. (Am. Chem. Soc., Div. Polym. Chem.)* **1990**, *31*(2), 263; *Macromolecules* **1991**, *24*, 132.
- (9) Lovinger, A. J.; Davis, D. D.; Schilling, F. C.; Bovey, F. A.; Zeigler, J. M. *Polym. Commun.* **1989**, *30*, 356.
- (10) Schilling, F. C.; Lovinger, A. J.; Zeigler, J. M.; Davis, D. D.; Bovey, F. A. *Macromolecules* **1989**, *22*, 3055.
- (11) Schilling, F. C.; Bovey, F. A.; Lovinger, A. J.; Zeigler, J. M. *Adv. Chem. Ser.* **1990**, No. 224, 341.
- (12) Jin, Y.; Wunderlich, B. *J. Therm. Anal.* **1990**, *36*, 765, 1519.
- (13) Ginnings, D. C.; Furukawa, G. T. *J. Am. Chem. Soc.* **1953**, *75*, 522.
- (14) A detailed description of the computations can be found in: (a) Cheban, Yu. V.; Lau, S.-F.; Wunderlich, B. *Colloid Polym. Sci.*, **1982**, *260*, 9. (b) Pan, R.; Varma-Nair, M.; Wunderlich, B. *J. Therm. Anal.* **1990**, *36*, 145.
- (15) Smith, A. L.; Anderson, D. R. *Appl. Spectrosc.* **1984**, *38*, 822.
- (16) Grebowicz, J.; Lau, S.-F.; Wunderlich, B. *J. Polym. Sci., Polym. Symp.* **1984**, *71*, 19.
- (17) Sverdlov, L. M. *Vibrational Spectra of Polyatomic Molecules*; Wiley Interscience: New York, 1973.
- (18) Varma-Nair, M.; Wesson, J. P.; Wunderlich, B. *J. Therm. Anal.* **1989**, *35*, 1913.
- (19) Pan, R.; Varma-Nair, M.; Wunderlich, B. *J. Therm. Anal.* **1989**, *35*, 955.
- (20) Pan, R. Y. L.; Cao, M.-Y.; Wunderlich, B. *J. Therm. Anal.* **1986**, *31*, 1319.
- (21) Gaur, U.; Wunderlich, B. *J. Phys. Chem. Ref. Data* **1981**, *10*, 119.
- (22) Jin, Y.; Wunderlich, B. *J. Phys. Chem.*, submitted.
- (23) Gaur, U.; Wunderlich, B. *Macromolecules* **1980**, *13*, 445.
- (24) Wunderlich, B.; Möller, M.; Grebowicz, J.; Baur, H. *Conformational Motion and Disorder in Low and High Molecular Mass Crystals*. *Adv. Polym. Sci.* **1988**, *87*.
- (25) Wunderlich, B.; Grebowicz, J. *Adv. Polym. Sci.* **1984**, *60/61*, 1.
- (26) Coker, T. G.; Wunderlich, B.; Janz, G. J. *Trans. Faraday Soc.* **1969**, *65*, 3361.
- (27) Wunderlich, B. *Macromolecular Physics, Vol. 3, Crystal Melting*; Academic Press: New York, 1980.
- (28) Weber, P.; Guillon, D.; Skoulios, A.; Miller, R. D. *J. Phys. Fr.* **1989**, *50*, 793.
- (29) Wunderlich, B.; Wiedemann, H. G. *Mol. Cryst. Liq. Cryst.* **1986**, *140*, 211.
- (30) Wiedemann, H. G.; Grebowicz, J. *Mol. Cryst. Liq. Cryst.* **1986**, *140*, 219.
- (31) Cao, M.-Y.; Wesson, J. P.; Loufakis, K.; Wunderlich, B. *Mol. Cryst. Liq. Cryst.* **1986**, *140*, 231.
- (32) Möller, M.; Oelfin, D.; Wunderlich, B. *Mol. Cryst. Liq. Cryst.* **1989**, *173*, 101.
- (33) Miller, K. J.; Grebowicz, J.; Wesson, J. P.; Wunderlich, B. *Macromolecules* **1990**, *23*, 1848.
- (34) Cao, M.-Y.; Varma-Nair, M.; Wunderlich, B. *Polym. Adv. Technol.* **1990**, *1*, 151.
- (35) Lyerla, J. R., Jr.; Levy, G. C. In *Topics in Carbon-13 NMR Spectroscopy*; Levy, G. C., Ed.; John Wiley & Sons: New York, 1974; Vol. 1.
- (36) Cheng, J.; Wunderlich, B., unpublished results.
- (37) Williams, E.; Sears, B.; Allerhand, A.; Cordes, E. H. *J. Am. Chem. Soc.* **1973**, *95*, 4871.
- (38) Levy, G. C. *J. Am. Chem. Soc.* **1973**, *95*, 6117.

**Registry No.** PDMSi, 28883-63-8; PDPSi, 96228-24-9; PDHSi, 94904-85-5; PTDSi, 107999-70-2; Cl<sub>2</sub>Me<sub>2</sub>Si (homopolymer), 30107-43-8; Cl<sub>2</sub>Si[(CH<sub>2</sub>)<sub>4</sub>Me]<sub>2</sub> (homopolymer), 97036-66-3; Cl<sub>2</sub>Si[(CH<sub>2</sub>)<sub>5</sub>Me]<sub>2</sub> (homopolymer), 97036-67-4; Cl<sub>2</sub>Si[(CH<sub>2</sub>)<sub>13</sub>Me]<sub>2</sub> (homopolymer), 117652-56-9.